

Research Paper
TMJ Disorders

Correlation between temporomandibular joint temporal component pneumatization and morphology: analysis by cone beam computed tomography

M. R. Nadaes, L. P. Lagos de Melo, F. Haiter Neto, D. Q. Freitas

Department of Oral Diagnosis, Division of Oral Radiology, Piracicaba Dental School, University of Campinas (UNICAMP), Piracicaba, São Paulo, Brazil

M. R. Nadaes, L. P. Lagos de Melo, F. Haiter Neto, D. Q. Freitas: Correlation between temporomandibular joint temporal component pneumatization and morphology: analysis by cone beam computed tomography. Int. J. Oral Maxillofac. Surg. 2019; 48: 779–786. © 2018 International Association of Oral and Maxillofacial Surgeons. Published by Elsevier Ltd. All rights reserved.

Abstract. The aim of this study was to evaluate whether a correlation exists between temporal bone pneumatization and the morphology of the articular eminence and glenoid fossa. A sample of 100 cone beam computed tomography scans was used, for a total of 200 temporomandibular joints (TMJ). Paracoronal and parasagittal images of the TMJ were evaluated by two examiners. For all TMJ, pneumatization was classified in the mid-lateral direction using a score of 0 or 1, and in the anteroposterior direction using a score ranging from 0 to 3. The inclination and height of the articular eminence and the thickness of the roof of the glenoid fossa were obtained. Pneumatization was found in the mid-lateral direction in 83.5% of the cases and in the anteroposterior direction in 88%. The age of the patient and side did not influence the prevalence or degree of pneumatization ($P = 0.051–0.953$), but female patients showed more pneumatization in the mid-lateral direction than male patients ($P = 0.014$). The presence of pneumatization did not affect articular eminence and mandibular fossa morphology. It is concluded that the presence and extent of pneumatization of the TMJ temporal component does not affect its morphology. However, professionals should be aware of the high prevalence of pneumatization and take this into account when performing TMJ assessment.

Key words: temporal bone; cone beam computed tomography; diagnostic imaging.

Accepted for publication 6 December 2018
Available online 27 December 2018

Mastoid pneumatization refers to air-filled cavities that occur when the epithelium infiltrates the developing temporal bone¹⁻³. The mastoid air cell system (MACS) is an extensive system of interconnecting air-filled cavities arising from the mastoid antrum and the middle ear⁴. The MACS can extend and affect other components of the temporal bone, such as the glenoid fossa and articular eminence, which form the temporomandibular joint (TMJ). The degree of pneumatization of temporal bone may therefore affect the temporal components of the joint⁵.

Pneumatization of the TMJ results in sites of minimal resistance, facilitating the spread of various pathological processes into the joint, infections, and fractures^{5,6}. As the TMJ is a complex structure⁷, the morphology of temporal bone is an important element in the biomechanics of the joint and masticatory system that interferes with the distribution of stresses in these regions⁸.

The features of the temporal bone are important for planning surgical procedures in this area. The temporal component of the joint often exhibits a variable pneumatization pattern and morphology, which can be a possible complicating factor in TMJ surgery⁹. Therefore, the bone component of the joint should be analyzed carefully during preoperative assessment and a variety of imaging modalities have been used for this purpose. Computed tomography (CT) is considered the method of choice for the assessment of bony structures and air spaces in the base of the skull⁹. Cone beam computed tomography (CBCT) is nowadays also used to evaluate the osseous components of the TMJ^{2,10}. This modality provides volumetric images with high spatial resolution, and the scan cost and radiation dose level are lower when compared to multidetector CT^{2,11-13}.

The individual variation in the temporal bone is significant and its degree of pneumatization is variable. Thus, temporal bone morphology features and the degree of temporal bone pneumatization could provide valuable information for TMJ assessment. Despite the importance of knowledge about the pneumatization and morphology of the temporal component of the TMJ, it appears that no studies in the literature have investigated whether TMJ pneumatization influences its morphology. Therefore, the aim of this study was to determine whether a correlation exists between temporal bone pneumatization and the morphology of the glenoid fossa and articular eminence using CBCT. Additionally, the authors propose a

classification of TMJ temporal component pneumatization based on its extent, for use in CBCT analysis.

Materials and methods

The study was approved by the local institutional research ethics committee.

Sample

The sample size was calculated in BioEstat version 5.3 software (Instituto de Desenvolvimento Sustentável Mamirauá, Tefé, MA, Brazil) and was based on the difference between the groups studied and their standard deviation, adopting a test power of 0.90. Ten CBCT scans that were not used in the final sample were evaluated to obtain these values, and it was calculated that a sample size of 48 would be required. In order to obtain enough data for each sex, examinations of 50 male and 50 female patients were selected. Therefore, the final sample consisted of 100 patients (age 20–60 years) who had undergone CBCT for the evaluation of the dentomaxillofacial region (for a total of 200 TMJs). CBCT scans that allowed complete visualization of the TMJ, zygomatic arch, articular eminence, glenoid fossa, external auditory canal, middle ear, and temporal bone mastoid process were included. CBCT scans with fractures, local surgical interventions, congenital craniofacial abnormalities, or pathological conditions, such as degenerative joint disease, were excluded.

All images were taken with an i-CAT Next Generation unit (Imaging Sciences International, Hatfield, PA, USA). The patients were asked to keep their teeth in maximum habitual intercuspation, with the Frankfort plane parallel to the horizontal plane and with the median sagittal plane perpendicular to the horizontal plane, according to the light indicators of the machine. The following CBCT acquisition protocol was used: field of view (FOV) of 13 × 16 cm, 37.07 mA, 120 kVp, voxel size of 0.25 mm, and scan time of 26 seconds with 360-degree rotation.

Images analysis

The datasets were evaluated using CS 3D Imaging Software, version 3.2.13 (Carestream Health, Inc., Atlanta, GA, USA), since the i-CAT software (XoranCAT, Xoran Technologies, Ann Arbor, MI, USA) does not calculate angular measurements. The images were analyzed on a 24.1-inch LCD monitor (MDRC-2124;

Barco, Kortrijk, Belgium) at a resolution of 1920 × 1200 pixels under reduced ambient light. Qualitative and quantitative analyses of the images were performed in consensus by two examiners with 6 years of experience in CBCT examinations, after a training session. The examiners were allowed to adjust brightness and contrast and to freely use the zoom tool.

Demographic information (sex and age) of the patients was recorded. Additionally, information was obtained for each side of the TMJ, including classification of TMJ temporal component pneumatization, inclination and height of the articular eminence, and thickness of the roof of the glenoid fossa.

Qualitative evaluation: TMJ temporal component pneumatization

Pneumatization of the temporal component was assessed in the anteroposterior and mid-lateral directions on parasagittal and paracoronal sections, respectively, by dynamic evaluation of CBCT scans. In the anteroposterior direction, four scores adapted from Zamaninaser et al.¹⁴ were used: score 0, MACS limited to the mastoid process; score 1, MACS extending beyond the mastoid process to the deepest point of the glenoid fossa; score 2, MACS extending beyond the deepest point of the glenoid fossa to the crest of the articular eminence (above the mandibular condyle); score 3, MACS extending beyond the crest of the articular eminence (Fig. 1). In the mid-lateral direction, two scores were used: score 0 (absent), MACS limited to the mastoid process or located medial to the medial wall of the glenoid fossa; score 1 (present), MACS located lateral to the medial wall of the glenoid fossa (Fig. 2).

Temporal component pneumatization was also classified as unilocular or multilocular according to Tyndall and Matteson¹. Unilocular pneumatization was identified as a single radiolucent oval air defect with well-defined bony borders. Multilocular pneumatization was identified as numerous radiolucent small air cavities.

Quantitative evaluation: TMJ temporal component morphology

For each TMJ, the long axis of the glenoid fossa was traced in its greatest mid-lateral extension from the axial reconstructed image of the CBCT scan (Fig. 3). This approach allowed a 0.25-mm thick paracoronal reconstruction of the central

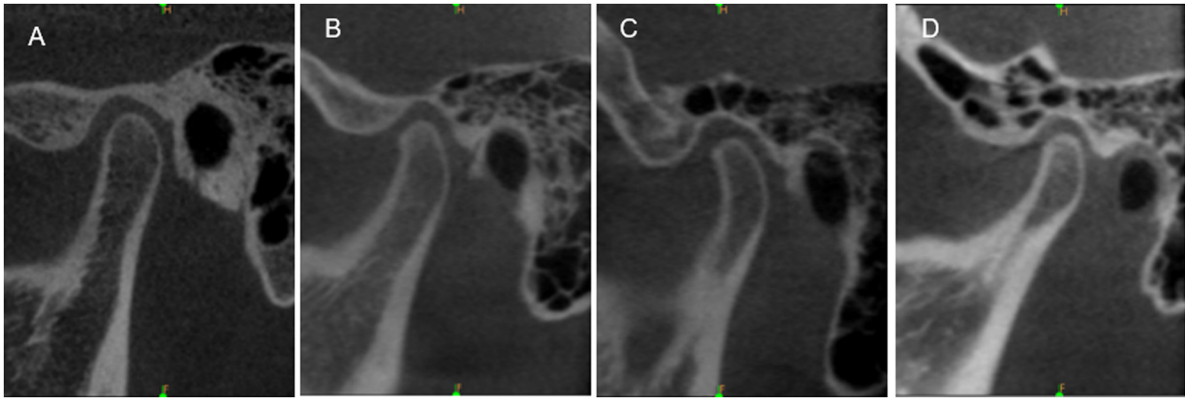


Fig. 1. Parasagittal reconstructions of cone beam computed tomography images showing the anteroposterior classification of TMJ temporal component pneumatization: (A) score 0; (B) score 1; (C) score 2; (D) score 3.

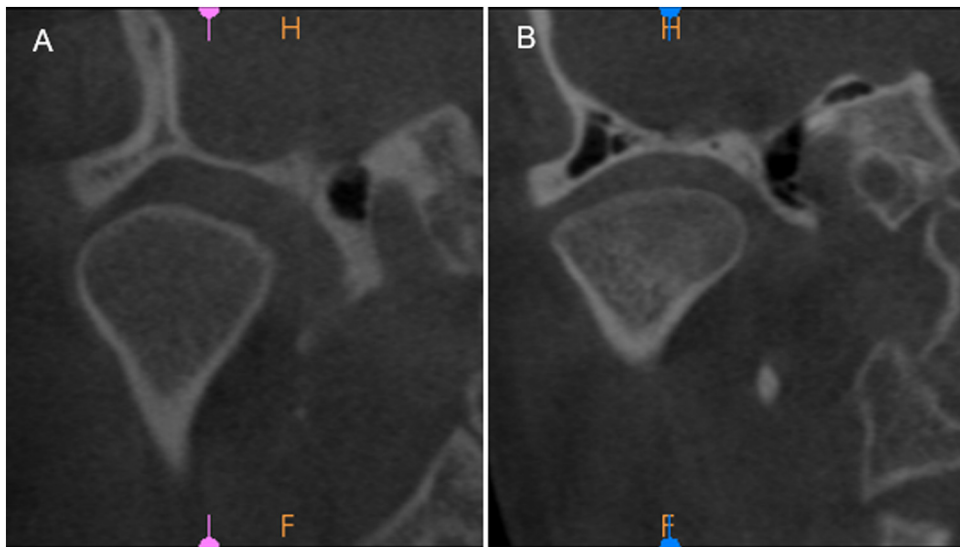


Fig. 2. Paracoronal reconstructions of cone beam computed tomography images showing the mid-lateral classification of TMJ temporal component pneumatization: (A) score 0 (absent); (B) score 1 (present).

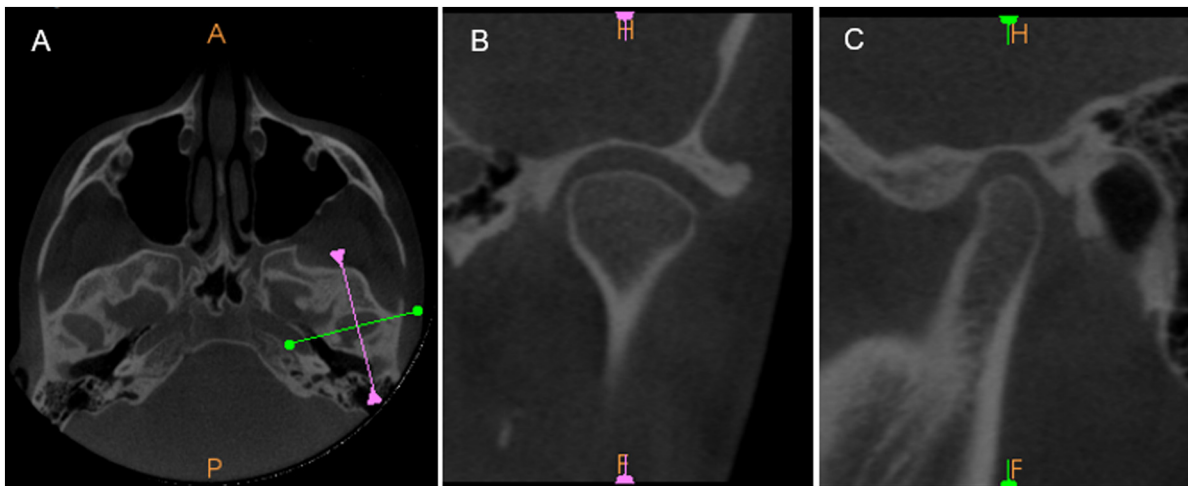


Fig. 3. (A) Axial reconstruction of a cone beam computed tomography image. To obtain the paracoronal reconstruction of the TMJ, the long axis of the glenoid fossa was traced in its greatest medial lateral extension. To obtain the parasagittal reconstruction, a line perpendicular to the paracoronal reference was drawn. (B) Paracoronal reconstruction. (C) Parasagittal reconstruction.

portion of higher dimension than the long axis of the glenoid fossa to be obtained. From this paracoronal reconstruction, secondary parasagittal reconstructed images were generated perpendicular to the long axis of the glenoid fossa at intervals of 1 mm. A 0.25-mm thick parasagittal reconstruction could thus be obtained from the central portion of the glenoid fossa.

For evaluation of the inclination and height of the articular eminence and thickness of the roof of the glenoid fossa, some anatomical landmarks adapted from Verner et al.¹⁵ and Ejima et al.¹⁶ were identified in the central reconstructed images of the TMJ: (1) articular eminence landmark: lowermost point of the articular eminence; (2) glenoid fossa landmark: uppermost point of the glenoid fossa; (3) middle cranial fossa landmark: point on the floor of the middle cranial fossa located in the thinnest part of the roof of the glenoid fossa.

From these anatomical landmarks, lines were defined in the central reconstructions of the TMJ for the quantitative measurements: (1) articular eminence line: line parallel to the horizontal plane, passing through the articular eminence landmark; (2) glenoid fossa line: line parallel to the horizontal plane, passing through the glenoid fossa landmark; (3) posterior surface of the articular eminence line: line tangent to the largest posterior surface of the articular eminence; (4) middle cranial fossa line: line parallel to the horizontal plane, passing through the middle cranial fossa landmark.

The inclination and height of the articular eminence were measured from these lines on the central parasagittal reconstruction of the TMJ. The inclination of the articular eminence in the anteroposterior direction was measured as the parasagittal angle (α) formed by the

intersection of the ‘articular eminence line’ with the ‘posterior surface of the articular eminence line’ (Fig. 4A). The parasagittal height (h) of the articular eminence was determined by measuring the perpendicular distance between the ‘articular eminence line’ and ‘glenoid fossa line’ (Fig. 4B).

The thickness of the roof of the glenoid fossa was measured on the central parasagittal and paracoronal reconstructions of the TMJ. The parasagittal thickness (PSth) and paracoronal thickness (PCth) of the roof of the glenoid fossa were determined as the perpendicular distance between the ‘glenoid fossa line’ and ‘middle cranial fossa line’ on parasagittal (Fig. 4C) and paracoronal reconstructions (Fig. 4D), respectively.

Thirty days after the first evaluation, 30% of the sample was reassessed to calculate intra-examiner agreement.

Statistical analysis

IBM SPSS Statistics version 22.0 (IBM Corp., Armonk, NY, USA) was used for the statistical analysis, adopting a significance level of 5%.

Multiple logistic regression was performed to verify whether sex, age, and side influenced the prevalence and degree of pneumatization in the anteroposterior and mid-lateral directions.

Normality of the parametric data was evaluated by Shapiro–Wilk test. Analysis of variance (one-way ANOVA) was used to compare the measurements found for the different degrees of pneumatization (score 0–3 for the anteroposterior direction and score 0 or 1 for the mid-lateral direction). The null hypothesis considered that there was no significant difference in the measurements between the different groups.

The weighted kappa test was performed to evaluate intra-examiner agreement for the categorical data, and the intra-class correlation coefficient (ICC) was used to calculate agreement for the parametric data.

Results

The weighted kappa test revealed excellent intra-examiner agreement for the classification of pneumatization (0.889 for anteroposterior direction; 0.965 for mid-lateral direction; 1.0 for locus classification), according to Landis and Koch¹⁷. The ICC also showed excellent reproducibility for the evaluation of the articular eminence (ICC = 0.985 for inclination and 0.994 for height) and roof of the glenoid fossa (ICC = 0.976 for parasagittal thickness and 0.937 for paracoronal thickness), according to Szklo and Nieto¹⁸.

The distribution of temporal bone pneumatization in the anteroposterior and mid-lateral directions according to sex and side is shown in Table 1. A high prevalence of pneumatization of TMJ components was observed (88% in the anteroposterior direction and 83.5% in the mid-lateral direction).

The degree of TMJ pneumatization according to age, for male and female patients, is presented in Table 2 (anteroposterior direction) and Table 3 (mid-lateral direction). According to multiple logistic regression (Table 4), the prevalence and degree of pneumatization in both directions was not influenced by side ($P = 0.374$ for anteroposterior and $P = 0.567$ for mid-lateral), or by age for the mid-lateral direction ($P = 0.953$); in the anteroposterior direction, the pneumatization was borderline correlated with patient age ($P = 0.051$). On the other hand, sex influenced the TMJ pneumatization in

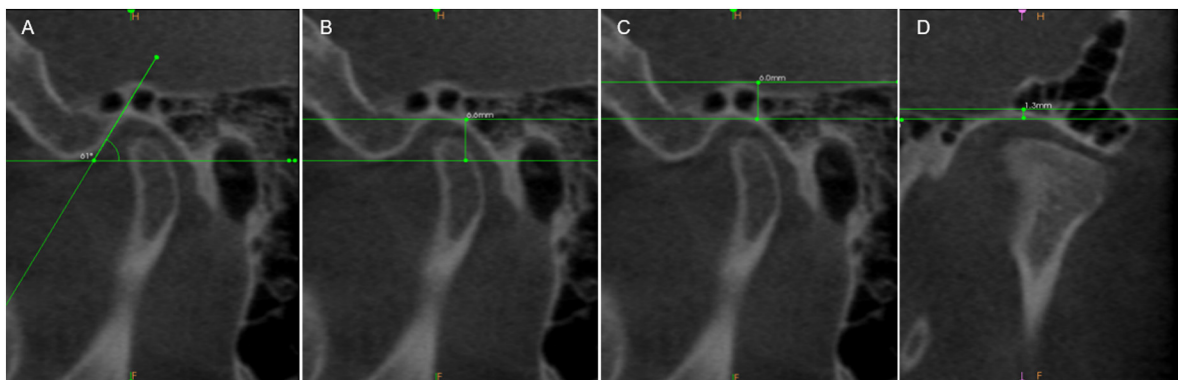


Fig. 4. Parasagittal and paracoronal reconstructions of cone beam computed tomography TMJ images showing: (A) parasagittal angle (α) of the articular eminence; (B) parasagittal height (h) of the articular eminence; (C) parasagittal thickness (PSth) of the roof of the glenoid fossa; (D) paracoronal thickness (PCth) of the roof of the glenoid fossa.

Table 1. TMJ pneumatization in the anteroposterior and mid-lateral directions according to sex and side.

Sex	Side	Anteroposterior direction, n (%)				Mid-lateral direction, n (%)	
		Score 0	Score 1	Score 2	Score 3	Score 0	Score 1
Male	Right	9 (37.5%)	19 (21.3%)	16 (23.9%)	6 (30%)	10 (30.3%)	40 (24.0%)
	Left	4 (16.7%)	22 (24.7%)	18 (26.9%)	6 (30%)	13 (39.4%)	37 (22.2%)
Female	Right	6 (25%)	24 (27.0%)	17 (25.4%)	3 (15%)	5 (15.2%)	45 (26.9%)
	Left	5 (20.8%)	24 (27.0%)	16 (23.9%)	5 (25%)	5 (15.2%)	45 (26.9%)
	Total	24 (12%)	89 (44.5%)	67 (33.5%)	20 (10%)	33 (16.5%)	167 (83.5%)

TMJ, temporomandibular joint.

Table 2. TMJ pneumatization in the anteroposterior direction according to age, for male and female patients.

Age (years)	Male		Female	
	n	%	n	%
20–29	18	18	32	32
Score 0	0	0	4	12.5
Score 1	7	38.9	12	37.5
Score 2	6	33.3	14	43.8
Score 3	5	27.8	2	6.2
30–39	12	12	14	14
Score 0	3	25	2	14.3
Score 1	2	16.7	7	50
Score 2	6	50	1	7.1
Score 3	1	8.3	4	28.6
40–49	34	34	24	24
Score 0	2	5.9	4	16.7
Score 1	19	55.9	10	41.7
Score 2	10	29.4	10	41.7
Score 3	3	8.8	0	0
50–60	36	36	30	30
Score 0	8	22.2	1	3.3
Score 1	13	36.1	19	63.3
Score 2	12	33.3	8	26.7
Score 3	3	8.3	2	6.7

TMJ, temporomandibular joint.

Table 3. TMJ pneumatization in the mid-lateral direction according to age, for male and female patients.

Age (years)	Male		Female	
	n	%	n	%
20–29	18	18	32	32
Score 0	3	16.7	4	12.50
Score 1	15	83.3	28	87.50
30–39	12	12	14	14
Score 0	4	33.3	1	7.1
Score 1	8	66.7	13	92.9
40–49	34	34	24	24
Score 0	5	14.7	5	20.8
Score 1	29	85.3	19	79.2
50–60	36	36	30	30
Score 0	11	30.6	0	0
Score 1	25	69.4	30	100

TMJ, temporomandibular joint.

the mid-lateral direction ($P = 0.014$), but did not influence the pneumatization in the anteroposterior direction ($P = 0.368$). In the mid-lateral direction, female patients

showed more score 1 (pneumatization) than male patients; additionally, multiple logistic regression indicated that female patients had an almost three times greater chance of presenting pneumatization than male patients (odds ratio = 2.702, Table 4).

Table 5 shows the mean linear and angular measurements of the articular eminence and glenoid fossa morphology according to the degree of pneumatization. ANOVA indicated that there were no differences in the measurements between the different degrees of pneumatization (all $P > 0.05$).

Following the classification proposed by Tyndall and Matteson¹, all cases of temporal bone pneumatization evaluated were classified as multilocular in this study.

Discussion

The morphology and degree of pneumatization of temporal bone provide important clinical information about the temporal component of the TMJ. Knowledge of these features is useful for the interpretation of imaging examinations and to understand the spread of pathological processes into the joint⁶. In addition, information about functional aspects and the development of the MACS and adjacent structures is essential to justify a certain surgical approach and predict post-surgical risks^{6,19}.

Pneumatization of the temporal bone is characterized by individual variation and by a multifactorial aetiology⁴. Additionally, advances in three-dimensional imaging have revealed a higher prevalence^{6,9,20} than that determined previously by two-dimensional radiography (1.0–2.6%)^{1,21}. Within this context, pneumatization of the temporal component of the TMJ has been considered an important anatomical variation. Since this joint is an anatomically and biomechanically complex structure⁷, many factors can affect its morphology or function. The TMJ allows a wide range of mandibular movements

and the transmission of forces and loads to the skull base²². Thus, a high mechanical load is transferred to the components of the temporal bone of this system⁸. Since the MACS in the TMJ temporal component represents an area of minimal resistance⁵, it was hypothesized that the degree of pneumatization of the temporal component of the joint may affect its morphology. This hypothesis was also based on CBCT examinations performed by the authors in daily practice, which suggested that pneumatization would occupy a large area in the TMJ temporal component, indicating some interference with TMJ morphology. In this context, it was observed that there was a tendency towards an increase in the thickness of the roof of the glenoid fossa when pneumatization reached that region (score 3), although without statistical significance.

Since classification of temporal bone pneumatization is difficult and complex and seems to vary among studies, it is proposed that the anatomical landmarks commonly employed in TMJ assessment are used to evaluate the extent of pneumatization by professionals and in future studies. The anteroposterior classification was based on that used by Zamaninaser et al.¹⁴, which seems to be a logical progression considering the temporal component of the joint. However, Zamaninaser et al.¹⁴ used the classification for panoramic radiographs, while the present authors propose its use for CBCT images. In this study, a classification was proposed that can easily be done in the views commonly obtained for evaluation of the TMJ, i.e., the parasagittal and paracoronal views. This approach appears to be more feasible than a previously proposed classification that uses axial reconstruction².

No significant correlation was found between the morphology and pneumatization of TMJ components, as demonstrated by the similar linear and angular measurements in the groups with different degrees of pneumatization. However, a high prevalence of pneumatization in the anteroposterior direction was observed, which was

Table 4. Multiple logistic regression for possible variables influencing the prevalence and degree of pneumatization.

Direction	Variables	Coefficient	P-value	OR	95% CI
Anteroposterior	Intercept	1.199	—	—	—
	Sex	0.156	0.368	1.169	0.49–2.79
	Age	–0.097	0.051	0.907	0.62–1.33
	Side	0.574	0.374	1.775	0.74–4.28
Mid-lateral	Intercept	0.527	—	—	—
	Sex	0.993	0.014	2.702	1.20–6.09
	Age	0.009	0.953	1.009	0.72–1.41
	Side	–0.224	0.567	0.799	0.37–1.71

OR, odds ratio; CI, confidence interval.

Table 5. Linear and angular measurements for the morphology of the articular eminence and glenoid fossa according to the degree of TMJ temporal component pneumatization; mean (standard deviation) values.

TMJ pneumatization		TMJ morphology			
Direction	Score	Articular eminence		Roof of glenoid fossa	
		Parasagittal angle (°)	Parasagittal height (mm)	Parasagittal thickness (mm)	Paracoronal thickness (mm)
Anteroposterior	0	53.58 (13.92)	5.94 (1.30)	1.50 (1.30)	0.97 (0.39)
	1	57.00 (13.04)	6.40 (1.53)	1.55 (1.26)	1.04 (0.62)
	2	57.85 (13.93)	6.62 (1.33)	1.73 (1.08)	1.20 (0.79)
	3	61.15 (12.79)	6.62 (1.69)	2.20 (1.51)	1.11 (0.51)
	P-value	0.306	0.239	0.165	0.361
Mid-lateral	0	51.67 (12.73)	6.27 (1.51)	1.74 (1.77)	1.08 (0.49)
	1	58.40 (13.34)	6.47 (1.46)	1.65 (1.11)	1.10 (0.69)
	P-value	0.080	0.467	0.713	0.916

TMJ, temporomandibular joint.

44.5% in the posterior part and 33.5% in the anterior part of the roof of the glenoid fossa (total 78%) and 10% in the articular eminence. Thus, the prevalence of TMJ temporal component pneumatization was 88% in the anteroposterior direction. Temporal bone pneumatization was also assessed in previous studies using CBCT scans and its prevalence ranged from 30.2% to 72%^{10,20} for pneumatization in the roof of the glenoid fossa and from 5% to 51.8%^{9,10,20} for pneumatization in the articular eminence. The divergence in the results can be explained by differences in the sample design, including the size and age group selected, as well as differences in CBCT units and acquisition protocols. Additionally, some differences in the anatomical landmarks used to classify the area of pneumatization were observed. The prevalence of TMJ temporal component pneumatization in the mid-lateral direction on paracoronal reconstructed images was 83.5%; however, no studies in the literature that classified mid-lateral TMJ temporal bone pneumatization using CBCT scans could be found.

The diagnosis of pneumatization is incidental since it has no clinical symptoms. Knowledge of its prevalence provides valuable information for understanding the dissemination of pathological processes into the MACS⁶. Tumours of the mastoid process and ear can extend

into the joint and may even result in ankylosis²³. In addition, the pneumatization of the temporal bone contributes to the absorption and dispersion of the kinetic energy of impact and to the protection of vital structures in the temporal bone in lateral trauma²⁴. Knowledge of TMJ temporal component pneumatization could also be used to determine the approach and the surgical management of the region^{6,19}, considering that the presence of these air cells is known to be a possible complicating factor during TMJ surgery²³.

Another important finding was the higher prevalence of pneumatization in the mid-lateral direction for female patients. The majority of previous studies did not find any difference between the sexes^{9,20}; however, these authors evaluated the pneumatization only in the anteroposterior direction, and this could explain the results, since the present study also did not find any difference between the sexes in the anteroposterior direction. This result means that the prevalence may not be different between the sexes, but that the area of pneumatization appears to be larger in females. With regard to clinical applicability, this difference between the pneumatization behaviours in anteroposterior and mid-lateral directions shows that it is important that professionals carefully look for air cells in

paracoronal reconstructions as well, in which MACS can be located lateral to the medial wall of the glenoid fossa. Therefore, this evaluation has demonstrated that the area of bone affected by pneumatization can be larger than professionals are used to seeing.

The results of this study showed a borderline correlation between pneumatization and age (indicated by a *P*-value of 0.051). However, the odds ratio was low, which means that the probability of pneumatization being present at one age rather than at others is low. This can be explained by the characteristic of pneumatization, which seems to be a developmental phenomenon, with the size increasing in three phases of life. The first stage occurs in the first year of life, in which there is rapid pneumatization. The second stage occurs between 1 and 6 years of age, in which the air cell area increases following a linear pattern. The third slower phase continues until puberty when the MACS reaches adult size²⁵. Since the study sample was aged between 20 and 60 years, the pneumatization had reached its adult size; thus, it was expected that age would not be a factor influencing the prevalence or degree of the pneumatization.

All cases of temporal bone pneumatization evaluated in this study were classified as multilocular by means of CBCT, in agreement with the results of a previous

study, which found a prevalence of 99.8% for glenoid fossa pneumatization and 96.6% for articular eminence pneumatization²⁰. Since CBCT provides images without superimposition, it exceeds the diagnostic accuracy of panoramic radiographs in the evaluation of temporal air cavities²⁰. The mechanism and factors influencing the pneumatization of the MACS are poorly understood⁴. The exclusively multilocular classification through CBCT images is an important finding, since this may help in understanding the mechanism of pneumatization and the continuity between these air cells.

The hypothesized correlation was not found in this study, i.e., there was no correlation between pneumatization of TMJ components and their morphology. However, the high prevalence of TMJ pneumatization is highlighted, which should be considered in cases of pathological processes at this site or during surgical planning. Moreover, as there were some difficulties in classifying pneumatization when the study was designed, a simple classification was developed to score the extent of pneumatization based on anatomical landmarks and reconstructed images that are usually examined in TMJ assessment.

In conclusion, the presence and extent of pneumatization in the temporal component of the TMJ does not affect its morphology. However, professionals should be aware of the high prevalence of pneumatization and take this into account when performing TMJ assessment, especially if a surgery is planned. In addition, a classification of pneumatization of the TMJ temporal component is proposed based on its extent in the anteroposterior and mid-lateral directions. It is recommended that professionals and researchers use this classification in CBCT images to compare and follow up their patients, to standardize research methods, and to compare results.

Funding

This work was partially financed by CAPES.

Competing interests

None.

Ethical approval

Local Institutional Research Ethics Committee (protocol # 58570716).

Patient consent

Not required.

References

1. Tyndall DA, Matteson SR. Radiographic appearance and population distribution of the pneumatized articular eminence of the temporal bone. *J Oral Maxillofac Surg* 1985;43:493–7.
2. Jadhav AB, Fellows D, Hand AR, Tadinada A, Lurie AG. Classification and volumetric analysis of temporal bone pneumatization using cone beam computed tomography. *Oral Surg Oral Med Oral Pathol Oral Radiol* 2014;117:376–84. <http://dx.doi.org/10.1016/j.oooo.2013.12.398>.
3. Lee DH, Kim MJ, Lee S, . Anatomical factors influencing pneumatization of the petrous apex. *Clin Exp Otorhinolaryngol* 2015;8:339–44. <http://dx.doi.org/10.3342/ceo.2015.8.4.339>.
4. Sethi A, Singh I, Agarwal AK, Sareen D. Pneumatization of mastoid air cells: role of acquired factors. *Int J Morphol [Internet]* 2006;24:35–8.
5. Al-Faleh W, Ibrahim ME. A tomographic study of air cell pneumatization of the temporal components of the TMJ in patients with temporomandibular joint disorders. *Egypt Dent J* 2005;51:1835–42.
6. Shamsad MP, Kamath G, Babshet M, Srikanth HS, Doddamani L. Prevalence of temporal bone pneumatization in relation to temporomandibular joint—a computed tomographic study. *J Stomatol Oral Maxillofac Surg* 2018;119:118–21. <http://dx.doi.org/10.1016/j.jormas.2017.11.016>.
7. Tamimi D, Jalali E, Hatcher D. Temporomandibular joint imaging. *Radiol Clin North Am* 2018;56:157–75.
8. Kranjcic J, Slaus M, Persic S, Vodanovic M, Vojvodic D. Differences in skeletal components of temporomandibular joint of an early medieval and contemporary Croatian population obtained by different methods. *Ann Anat* 2016;203:52–8. <http://dx.doi.org/10.1016/j.aanat.2015.03.004>.
9. Miloglu O, Yilmaz AB, Yildirim E, Akgul HM. Pneumatization of the articular eminence on cone beam computed tomography: prevalence, characteristics and a review of the literature. *Dentomaxillofac Radiol* 2011;40:110–4. <http://dx.doi.org/10.1259/dmfr/75842018>.
10. İlgüy M, Dölekoğlu S, Fişekçioğlu E, Ersan N, İlgüy D. Evaluation of pneumatization in the articular eminence and roof of the glenoid fossa with cone-beam computed tomography. *Balkan Med J* 2015;32:64–8. <http://dx.doi.org/10.5152/balkan-medj.2015.15193>.
11. Barghan S, Tetradis S, Mallya SM. Application of cone beam computed tomography for assessment of the temporomandibular joints. *Aust Dent J* 2012;57:109–18. <http://dx.doi.org/10.1111/j.1834-7819.2011.01663.x>.
12. Nascimento HAR, Andrade MEA, Frazão MAG, Nascimento EHL, Ramos-Perez FMM, Freitas DQ. Dosimetry in CBCT with different protocols: emphasis on small FOVs including exams for TMJ. *Braz Dent J* 2017;28:511–6. <http://dx.doi.org/10.1590/0103-6440201701525>.
13. Parsa A, Ibrahim N, Hassan B, Motroni A, van der Stelt P, Wismeijer D. Reliability of voxel gray values in cone beam computed tomography for preoperative implant planning assessment. *Int J Oral Maxillofac Implants* 2012;27:1438–42.
14. Zamaninaser A, Rashidipoor R, Mosavat F, Ahmadi A. Prevalence of zygomatic air cell defect: panoramic radiographic study of a selected Esfehanian population. *Dent Res J (Isfahan)* 2012;9:S63–8.
15. Verner FS, Roque-Torres GD, Ramírez-Sotello LR, Devito KL, Almeida SM. Analysis of the correlation between dental arch and articular eminence morphology: a cone beam computed tomography study. *Oral Surg Oral Med Oral Pathol Oral Radiol* 2017;124:420–31. <http://dx.doi.org/10.1016/j.oooo.2017.07.004>.
16. Ejima K, Schulze D, Stippig A, Matsumoto K, Rottke D, Honda K. Relationship between the thickness of the roof of glenoid fossa, condyle morphology and remaining teeth in asymptomatic European patients based on cone beam CT data sets. *Dentomaxillofac Radiol* 2013;42:90929410. <http://dx.doi.org/10.1259/dmfr/90929410>.
17. Landis JR, Koch GG. The measurement of observer agreement for categorical data. *Biometrics* 1977;33:159–74.
18. Szklo R, Nieto FJ. Epidemiology beyond the basis. *Aspen Publ* 2000:343–404.
19. Ars B, Dirckx J, Ars-Piret N, Buytaert J. Insights in the physiology of the human mastoid: message to the surgeon. *Int Adv Otol* 2012;8:296–310.
20. Ladeira DB, Barbosa GL, Nascimento MC, Cruz AD, Freitas DQ, Almeida SM. Prevalence and characteristics of pneumatization of the temporal bone evaluated by cone beam computed tomography. *Int J Oral Maxillofac Surg* 2013;42:771–5. <http://dx.doi.org/10.1016/j.ijom.2012.12.001>.
21. Kaugars GE, Mercuri LG, Laskin DM. Pneumatization of the articular eminence of the temporal bone: prevalence, development, and surgical treatment. *J Am Dent Assoc* 1986;113:55–7.
22. Kranjčić J, Vojvodić D, abarović D, Vodanović M, Komar D, Mehulić K. Differences in articular-eminence inclination between medieval and contemporary human populations. *Arch Oral Biol* 2012;57:1147–52. <http://dx.doi.org/10.1016/j.archoralbio.2012.05.009>.
23. Groell R, Fleischmann B. The pneumatic spaces of the temporal bone: relationship to the temporomandibular joint. *Dentomax-*

- illofac Radiol* 1999;**28**:69–72. <http://dx.doi.org/10.1038/sj/dmfr/4600414>.
24. Ilea A, Butnaru A, Sfrângeu SA, Hedeşiu M, Dudescu CM, Berce P, Chezan H, Hurubeanu L, Trombiş VE, Câmpian RS, Albu S. Role of mastoid pneumatization in temporal bone fractures. *AJNR Am J Neuroradiol* 2014;**35**:1398–404. <http://dx.doi.org/10.3174/ajnr.A3887>.
25. Cinamon U. The growth rate and size of the mastoid air cell system and mastoid bone: a review and reference. *Eur Arch Otorhinolaryngol* 2009;**266**:781–6. <http://dx.doi.org/10.1007/s00405-009-0941-8>.

Address:
Mariana Rocha Nadaes
University of Campinas
Piracicaba Dental School

Department of Oral Diagnosis
Av. Limeira
901
13414-903
Piracicaba
São Paulo
Brazil
Tel.: +55 19 2106 5327
E-mail: mnrnadaes@gmail.com